# RELATIVE CONTRIBUTION OF SURFACE ROUGHNESS AND BOTTOM ATTENUATION TO PROPAGATION LOSS IN SHALLOW WATER

W. A. Kuperman

F. Ingenito

Naval Research Laboratory, Washington, D. C. 20375

## Abstract

A simulation study has been performed to investigate the relative importance of the contributions of surface roughness and bottom attenuation to propagation loss under differing environmental conditions. The NRL normal mode model, which was used in the calculations, is restricted to range independent environments but can accommodate a sound velocity profile in the water layer which varies arbitrarily with depth. The bottom sediment is treated as a fluid of constant density and sound velocity with a small frequency dependent attenuation coefficient. The surface of the water layer is allowed to be rough and by using an ocean surface wave spectrum model, the roughness is characrerized by a wind speed and wind direction. Modal attenuation coefficients have been calculated as a function of frequency and parameterized according to bottom sediment type, velocity profile and wind direction. Propagation loss at a given range has been calculated as a function of wind velocity, where frequency, sediment type and velocity profile were varied. The results show that for isovelocity and downward refracting profiles the contribution of surface roughness to the total propagation loss is important when the wind speed exceeds a threshold value, the latter depending upon the environmental conditions. Surface roughness can be the major attenuation mechanism for upward refracting profiles above a certain windspeed.

## INTRODUCTION

Aside from cylindrical spreading, the major contributions to propagation loss in shallow water are bottom attenuation and boundary roughness. In this study we theoretically investigate the relative importance of bottom loss and surface roughness in different shallow water acoustic environments using a normal mode model.[1] In a duct where there are no loss mechanisms (other than geometric spreading) the eigenvalues associated with a normal mode solution are real. The introduction of loss mechanisms results in complex eigenvalues, the imaginary parts of which can be interpreted as attenuation coefficients of the individual normal modes. Rather than directly solve a complex eigenvalue problem, expressions for attenuation coefficients due to bottom loss can be derived which relate the imaginary parts of the eigenvalues to the solutions of the lossless normal mode problem.[2] For the rough surface case, an impedance boundary condition[3] which has been derived earlier can be used to calculate the resulting imaginary parts of the eigenvalues. In the next section we outline the derivation of these attenuation coefficients. In Section II we present some calculated results using a wind driven model of a fully developed sea to describe the surface roughness and some empirical results on ocean bottom sediments to describe the bottom loss.

## I. THEORY

Figure 1 illustrates the geometry. A harmonic point source of unit source strength is located on the z axis at depth $z_0$ and it is desired to calculate the sound field at the point (x,y,z). If $\phi(x,y,z)$ is the velocity potential then we must have (a time dependence of $\exp(-i\omega t)$ is assumed)

$$\nabla^2\phi(x,y,z) + \left[\omega^2/c^2(z)\right]\ \phi(x,y,z) = -\ \delta^2(\vec{r})\delta(z-z_0), \tag{1}$$

where $\vec{r}$ is a transverse vector to the point (x,y). The boundary conditions associated with Eq. 1 are that $\phi$ vanishes at the surface and that the pressure and particle velocity are continuous at the ocean bottom water-sediment interface. It is convenient to solve Eq. 1 using a Fourier transform method with

$$\phi(\vec{r},z) = \frac{1}{2\pi}\int d\vec{\eta}\ e^{i\vec{\eta}\cdot\vec{r}}\ v(\vec{\eta},z), \tag{2}$$

where $\vec{\eta}$ is the two dimensional Fourier conjugate vector of $\vec{r}$ and $v(\vec{\eta},z)$ satisfies the inhomogeneous differential equation

$$\frac{d^2v}{dz^2} + \left[\omega^2/c^2(z) - \eta^2\right]\ v = -\ \frac{1}{2\pi}\ \delta(z-z_0). \tag{3}$$

We seek the normal mode solution of Eq. 3 in terms of the eigenfunctions, $v_n$, and the eigenvalues, $k_n$, of the homogeneous form of Eq. 3,

$$\frac{d^2v_n}{dz^2} + \left[k^2(z)-k_n^2\right]\ v_n = 0, \tag{4}$$

where $k^2(z) = \omega^2/c^2(z)$. The solution to Eq. 1, neglecting the continuous modes, is then given by

$$\phi(\vec{r},z) = \frac{-\rho_1}{(2\pi)^2} \sum_n \int d\vec{\eta} \; \frac{v_n(z_0)v_n(z)}{k_n^2 - \eta^2} \; e^{i\vec{\eta}\cdot\vec{r}} \tag{5}$$

The contour is appropriately chosen to give outgoing waves. Note that the poles in the integrand correspond to a summation of integral representations of Hankel functions. When no attenuation mechanisms are present, the $k_n$'s are real and hence the poles are located on the real axis. When loss is introduced, the eigenfunctions and eigenvalues become complex. In particular, $k_n \rightarrow k_n + i\delta_n$ and the dominant effect on Eq. 5 is to shift the poles off the real axis. The asymptotic form of the Hankel function is proportional to $\exp(ik_n r)$ and hence, when $k_n$ has an imaginary part, each term in the normal mode expansion will contain an attenuation coefficient $\exp(-\delta_n r)$.

The complex conjugates of $v_n$ and $k_n$, $v_n^*$ and $k_n^*$, satisfy the complex conjugated version of Eq. 4. By manipulating Eq. 4 and its complex conjugate it has been shown[3] that one can (under reasonable assumptions) derive an expression for $\delta_n$ without going through the formal solution of a complex eigenvalue problem.

When the sole attenuation mechanism is bottom attenuation and the propagation constant of a plane wave in the bottom can be written as a complex number of the form $\omega/c_2+i\varepsilon$ where $c_2$ is the velocity of sound in the bottom, then the imaginary parts of the normal mode eigenvalues (the attenuation coefficients) are given by[2]

$$\delta_n^B \approx \varepsilon\gamma_n, \tag{6}$$

where

$$\gamma_n = \frac{\omega\rho_2}{c_2 k_n} \int_H^\infty |v_n(z)|^2 \, dz. \tag{7}$$

If the ocean surface is rough, an additional loss mechanism for the mean acoustic field is introduced. For random roughness of the ocean surface we can replace the pressure release condition at the actual surface $z=\alpha(\vec{r})$ where $\alpha$ is a random function by an effective impedance boundary condition at the mean surface $z=0$.[3] This new boundary condition for the mean field is

$$v = i\,\langle\alpha^2\rangle\, a(\vec{\eta})\, \frac{\partial v}{\partial z}, \tag{8}$$

where

$$a(\vec{\eta}) = \frac{1}{2\pi} \int d\vec{\xi} \; \sqrt{k^2(0) - \xi^2} \; P(\vec{\eta}-\vec{\xi}). \tag{9}$$

$P(\vec{\lambda})$ is the normalized power spectrum of the ocean surface, i.e., the Fourier transform of the autocorrelation function of the ocean surface.

Using a method similar to that used for the bottom loss case, we can again derive expressions for the imaginary parts of the eigenvalues without going through a formal solution of a complex eigenvalue problem. The derivation will be given elsewhere; below we give the result:

$$\delta_n^s(\vec{\eta}) = -(4ik_nA_n)^{-1} \left| v_n^1(0) \right|^2 \left[ \frac{v_n^*(0)}{v_n^{*\prime}} - \frac{v_n(0)}{v_n'(0)} \right], \tag{10}$$

with the prime denoting the z derivative and where $A_n$ is a normalization integral,

$$A_n = \int_0^\infty dz\rho(z) \left| v_n(z) \right|^2. \tag{11}$$

The values of the logarithmic derivatives of the velocity potentials are given by Eq. 8 and its complex conjugate. Returning to the dispersion expression in the denominator of Eq. 5 we see that the poles now occur at

$$\eta = k_n + i\delta_n^s(\eta) \approx k_n + i\delta_n^s(k_n), \tag{12}$$

the last approximation resulting from the fact that $\delta_n^s$ is of the order $\alpha^2$ which is our perturbation expansion parameter. The attenuation coefficient due to surface roughness is therefore given by

$$\delta_n^s = \frac{<\alpha^2>}{2k_nA_n} \left| v_n'(0) \right|^2 \mathrm{Re}\left\{ a(k_n) \right\} \tag{13}$$

Finally, the normal mode attenuation coefficient resulting from both bottom loss and surface scattering is given by the sum of the two individual coefficients,

$$\delta_n = \delta_n^B + \delta_n^s. \tag{14}$$

## II. SAMPLE CALCULATIONS

In this section we present some computer results using different environmental inputs to calculate transmission loss (TL). If we carry out the integration in Eq. 5 and insert the asymptotic form of the Hankel function into the expression we get that the acoustic pressure is given by

$$P \approx \frac{\omega\rho_1}{\sqrt{8\pi r}} \sum_{n=1}^{N} \frac{v_n(z_0)v_n(z)}{\sqrt{k_n}} \exp(ik_n r) \exp(-\delta_n r) \tag{15}$$

where $\delta_n$ is given by Eq. 14. The acoustic field at a receiver is, of course, a function of receiver depth. Since we are concerned here with attenuation we can average out the effect of receiver depth by defining our transmission loss as follows:

$$TL = 10 \log \left\{ \frac{1}{M} \sum_{m=1}^{M} P_m^2 \right\}, \tag{16}$$

where $P_m$ is the pressure at the m-th receiver and M is the number of receivers; for the cases that follow we will take M=10 with the receivers equally spaced throughout the water column. Finally, as a measure of attenuation we define the function $\Gamma$ at range R to be

$$\Gamma = R^{-1} \left[ TL \text{ (windspeed} \neq 0) - TL \text{ (windspeed} = 0) \right] . \tag{17}$$

$\Gamma$ will be expressed in dB/km and is a function of surface roughness; $\Gamma$ is a measure of attenuation due to surface loss with geometric spreading loss and bottom loss eliminated. It is, unfortunately, a range dependent quantity but at a given range, it is indicative of the importance of surface loss.

We now present some numerical calculations of this $\Gamma$ function for different shallow water environments. Below are the three bottom types used which were taken from Hamilton's work.[4,5]

PROPERTIES OF THE THREE BOTTOM SEDIMENTS

| | SOUND SPEED RATIO ($C_2/C_1$) | DENSITY ($\rho_2$) | K |
|---|---|---|---|
| A. COARSE SAND | 1.201 | 2.03 | 0.46 |
| B. SILTY SAND | 1.096 | 1.83 | 0.65 |
| C. SAND-SILT-CLAY | 1.032 | 1.58 | 0.2 |

K is defined in Hamilton's paper[4] by the relation $\alpha$(dB/m) = Kf(kHz) where $\alpha$ is the attenuation constant for a plane wave traveling through the bottom sediment.

Three generic sound speed profiles chosen for the calculations are shown in Fig. 2. Note that the depth of water was taken to be 100 meters in all the cases.

We mentioned earlier that $\Gamma$ is range dependent. We show this range dependence for a typical case in Fig. 3. The Pierson-Moskowitz[5] spectrum for a wind generated fully developed sea is used as our model for the ocean surface roughness. The calculations were done for three different source depths. In the following examples we present some sample results using 50 meters as the source depth and 25 km as the range.

Figures 4 and 5 are samples of the results at 50 Hz. Note that cases II are for negative profiles. Case IIA and IIB indicate a saturation effect after a certain wind velocity is reached. Cases IIA and IIB have four and three normal modes, respectively, of which only one in each case is trapped below the thermocline. Because the other modes that interact with the surface are stripped away we are just left with the trapped modes which do not interact with the surface. Hence, we have this saturation effect. Case IIC only has one mode that is barely trapped below the thermocline and therefore no surface loss should be observed.

Figure 5 illustrates the results for an upward refracting profile. Note that there is no saturation effect. Case C is significantly different than cases A and B indicating the importance of bottom type when calculating surface loss.

Figures 6 through 11 are sample results at 500 Hz. These figures include the effect of wind direction relative to the direction of acoustic propagation. The calculated results indicate a larger surface loss along the direction of the wind.

Figures 8 and 9 are for negative profiles and again we see the saturation effect. However, saturation occurs at a lower windspeed and at a significantly higher level than at 50 Hz. No saturation effects are predicted in Figs. 6 and 7 which are for isovelocity or Figs.10 and 11 which are for an upward refracting profile. For all these cases the surface loss is significant as compared to bottom loss. The transmission loss with bottom attenuation was of the order of 70 dB with 5 to 10 dB being attributed to bottom loss. For the isovelocity case for windspeeds greater than about 10 m/sec the contribution to transmission loss begins to exceed 5 dB at this 25 km range. For the upward refracting case, the surface loss is much larger.

A few general conclusions can be made from this limited sample of results. For negative gradient profiles we see a saturation effect. The fact that $\Gamma$ climbs very rapidly to its saturated value indicates that a simple surface scattering model could be used in some transmission loss programs for negative gradient cases which is certainly typical of many areas of the world. This model would be a threshold model putting in no surface loss below a certain windspeed and a constant value above this critical windspeed. For the positive gradient cases both at 50 and 500 Hz, surface loss was a significant contribution to the total transmission loss being of the order of the bottom loss in the 50 Hz case and the dominating loss mechanism for 500 Hz. Finally, we have seen examples when the bottom type has a significant effect on surface loss.

An important caveat must be mentioned. These results are for a Pierson-Moskowitz model of a wind driven fully developed sea. Calculations must be made for more realistic ocean surfaces and work is continuing along that direction together with doing more calculations for higher frequency cases.

The work is being supported by NAVSEA 06H1-4 and the Office of Naval Research.

REFERENCES

1. J. F. Miller and F. Ingenito, "Normal Mode FORTRAN Program for Calculating Sound Propagation in the Ocean," NRL Memo Report 3071, June 1975.

2. F. Ingenito, J. Acoust. Soc. Am. 53, 858 (1973).

3. W. A. Kuperman, J. Acoust. Soc. Am. 58, 365 (1975).

4. E. L. Hamilton, Geophysics 37, 620 (1972).

5. E. L. Hamilton, J. Geophys, Res. 23, 4423 (1970).

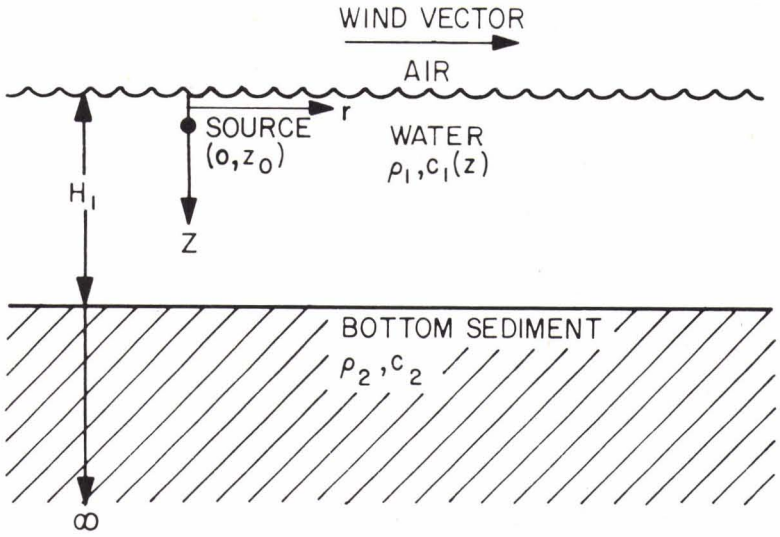


FIG. 1

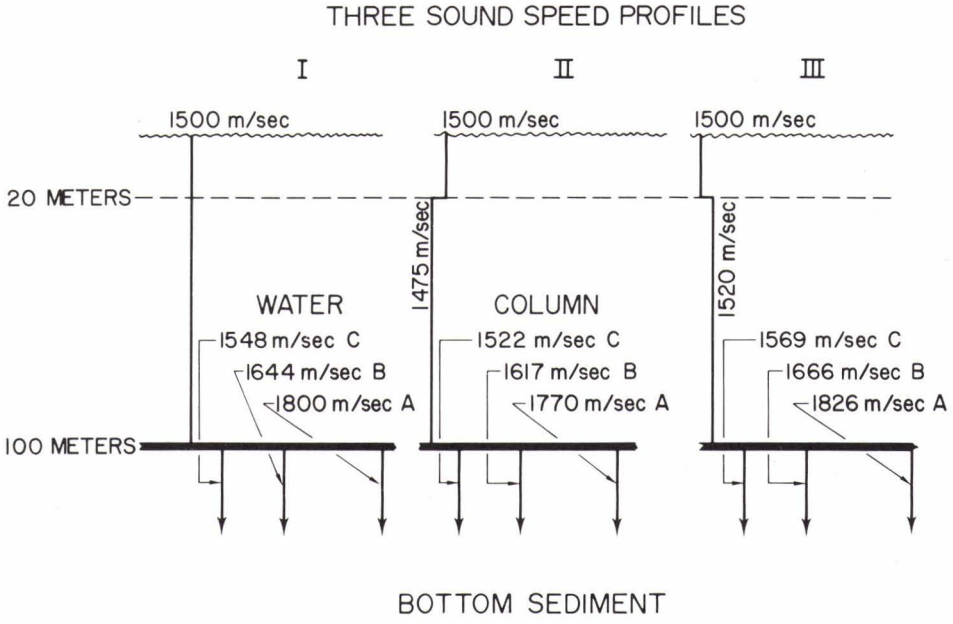


FIG. 2

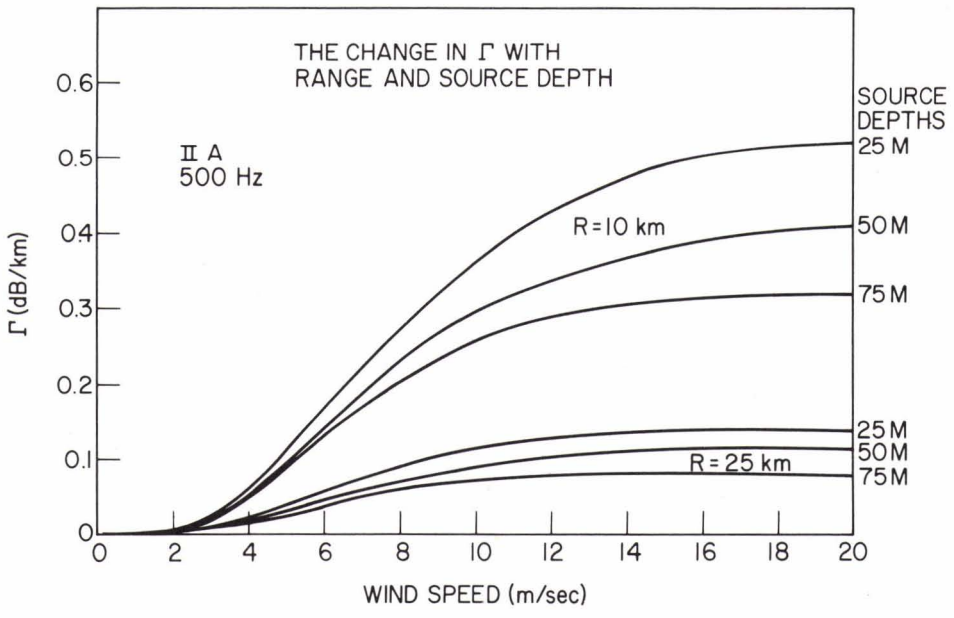


FIG. 3

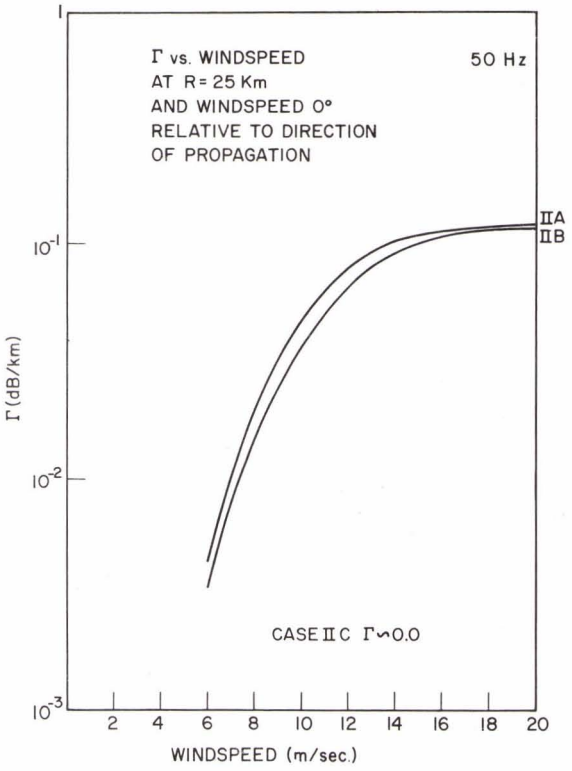


FIG. 4

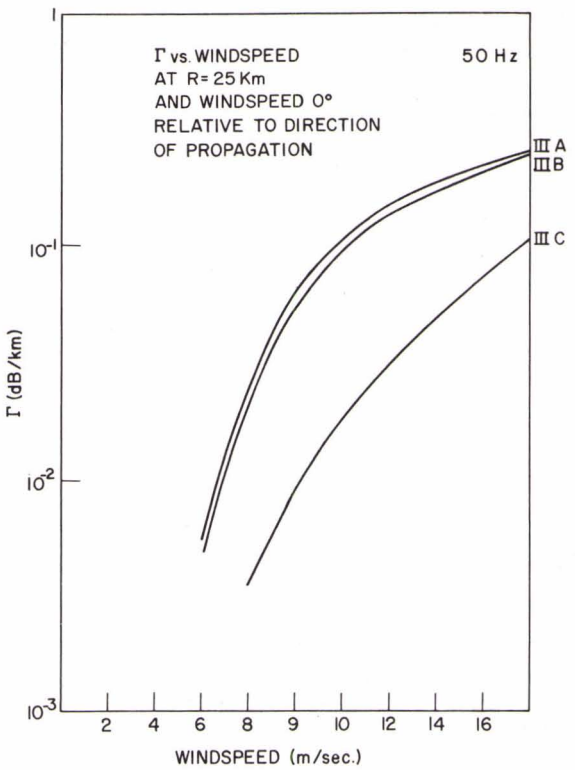


FIG. 5

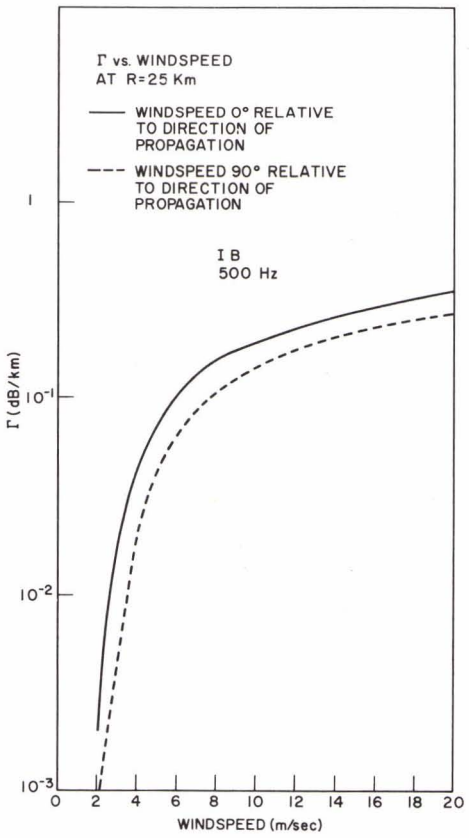


FIG. 6

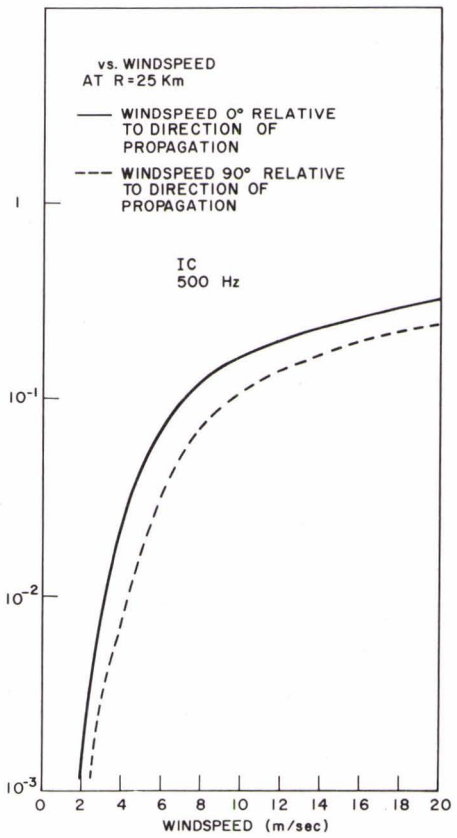


FIG. 7

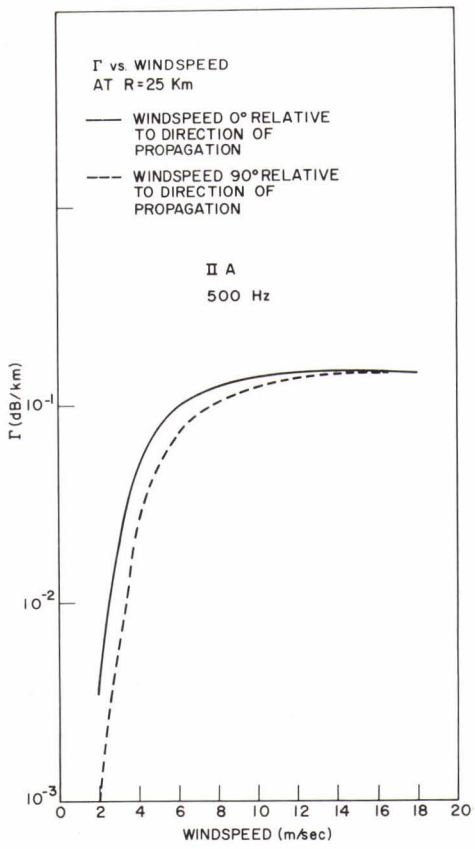


FIG. 8

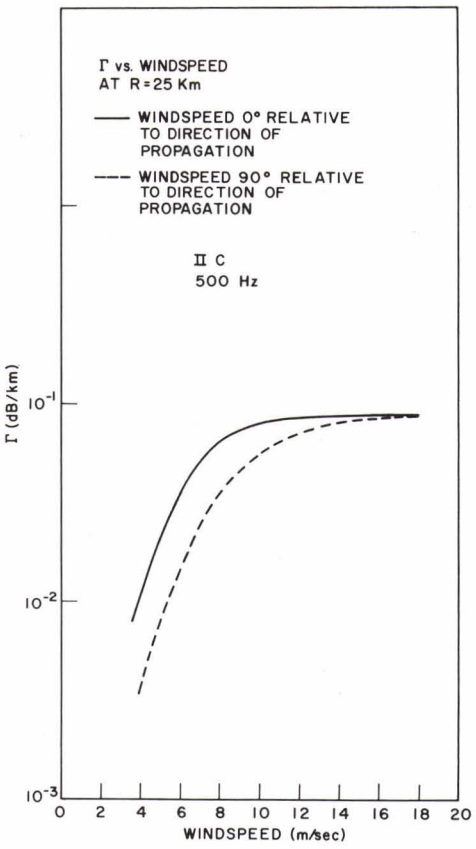


FIG. 9

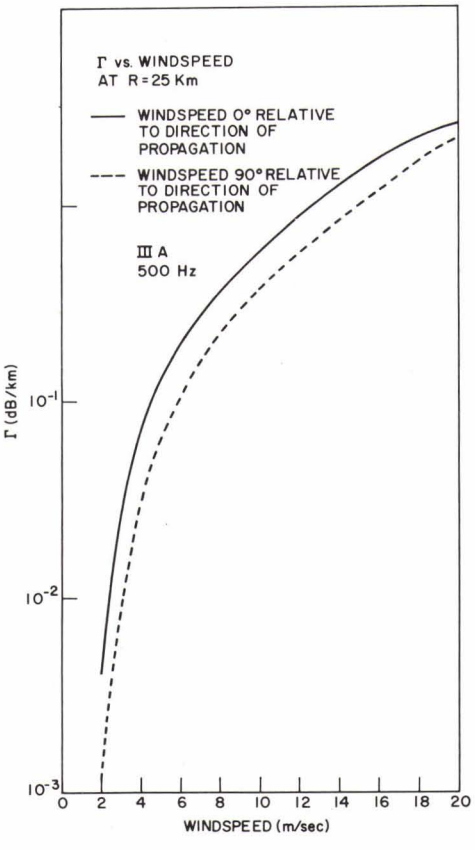


FIG. 10

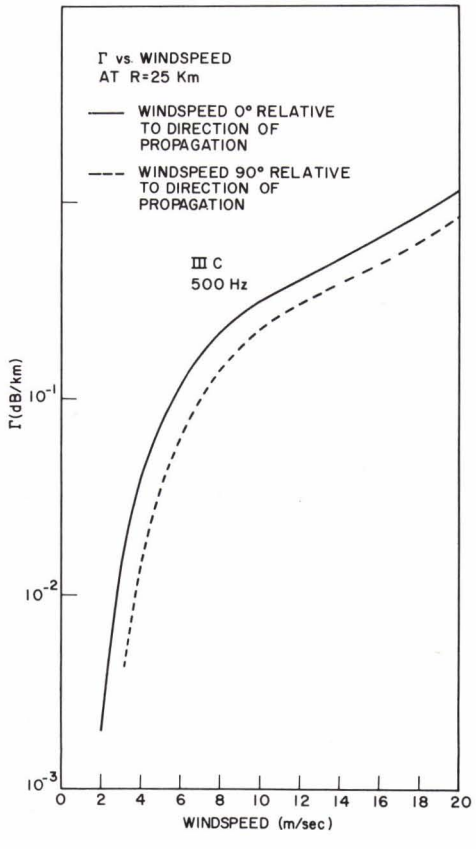


FIG. 11